

In terms of the eigenfunction expansion, the solution is

$$\begin{aligned}
 w(z, t) = & \sum_{n=0}^{\infty} B_n f_n(z) \int_0^t q(t - \tau) \\
 & \times \exp - (if\tau) \exp - \left[ \lambda_n \int_{t-\tau}^t \eta(\theta) d\theta \right] d\tau \\
 & + \frac{F(t)}{\eta(t)} w_s(z) - \frac{F(t)}{\eta(t)} \sum_{n=0}^{\infty} D_n f_n(z) \\
 & + \sum_{n=0}^{\infty} (if + \lambda_n) D_n f_n(z) \int_0^t F(t - \tau) \\
 & \times \exp - (if\tau) \exp - \left[ \lambda_n \int_{t-\tau}^t \eta(\theta) d\theta \right] d\tau
 \end{aligned}$$

[which replaces Eq. (7) of Jordan and Baker (1980a)] where  $w_s(z)$ ,  $f_n(z)$ ,  $\lambda_n$ ,  $B_n$  and  $D_n$  are the same as before.

**Acknowledgment.** Part of this work was supported by the U.S. Environmental Protection Agency, Grant R805667-01-0.

## REFERENCES

- Baker, J. R., and T. F. Jordan, 1980: Vertical-structure functions for time-dependent flow in a well-mixed fluid with turbulent boundary layers at the bottom and top. *J. Phys. Oceanogr.*, **10**, 1691-1694.
- Csanady, G. T., and P. T. Shaw, 1980: The evolution of a turbulent Ekman layer. *J. Geophys. Res.*, **85**, 1537-1547.
- Forristall, G. Z., 1974: Three-dimensional structure of storm-generated currents. *J. Geophys. Res.*, **79**, 2721-2729.
- Jelesnianski, C. P., 1970: Bottom stress time history in linearized equations of motion for storm surges. *Mon. Wea. Rev.*, **98**, 462-478.
- Jordan, T. F., and J. R. Baker, 1980a: Vertical structure of time-dependent flow dominated by friction in a well-mixed fluid. *J. Phys. Oceanogr.*, **10**, 1091-1103.
- , and —, 1980b: Current as a function of depth in the water: Solution of a linear model. U.S. Environ. Protection Agency Tech. Rep.
- Madsen, O. S., 1977: A realistic model of the wind-induced Ekman boundary layer. *J. Phys. Oceanogr.*, **7**, 248-255.
- Nihoul, J. C. J., 1977: Three-dimensional model of tides and storm surges in a shallow well-mixed continental sea. *Dyn. Atmos. Oceans*, **2**, 29-47.
- Thomas, J. H., 1975: A theory of steady wind-driven currents in shallow water with variable eddy viscosity. *J. Phys. Oceanogr.*, **5**, 136-142.

## A Deep, Thick, Isopycnal Layer within an Anticyclonic Eddy

ZACHARIAH R. HALLOCK,<sup>1</sup> WILLIAM J. TEAGUE AND ROBERT D. BROOME

U.S. Naval Oceanographic Office, NSTL Station, MS 39522

27 April 1981 and 8 September 1981

### ABSTRACT

An anticyclonic mesoscale eddy, encountered during a hydrographic survey in the Sargasso Sea in September 1979, is described. Embedded in the eddy at a depth of 800 m was an isopycnal lens of anomalous water which extended 150 m vertically and ~40 km horizontally. The source of the lens is not known but may be related to frontal processes in the area.

### 1. Introduction

In August, 1979, a hydrographic survey was conducted in the Sargasso Sea near 31°N, 72°30'W by the U.S. Naval Oceanographic Office aboard USNS *Kane*. The survey consisted of a grid of CTD (conductivity-temperature-depth) stations and XBT (expendable bathythermograph) drops over an area of ~100 n mi square. A total of 31 CTD stations were occupied and 150 XBT drops were made.

Analysis of data revealed an anticyclonic eddy embedded in a larger anticyclonic field. Also present was a surface front just west of the eddy and oriented

roughly north-south. Most notable was a peculiar lens of homogeneous water in the main thermocline near the center of the eddy.

### 2. Observations

Data were acquired with a Neil Brown Instrument Systems Mark III CTD and with Sippican T-7 XBT probes. CTD data were recorded directly on computer-compatible magnetic tape and XBT data on digital cassettes.

Separation of CTD stations was 20 n mi on the first, third and fifth east-west transects (see Fig. 1) and 40 n mi on the remainder. XBT drops were made every 10 n mi. Most CTD casts were to a depth of 2000 m; several were to the bottom, ~5000 m.

<sup>1</sup> Present affiliation: Naval Ocean Research and Development Activity, NSTL Station, MS 39529.

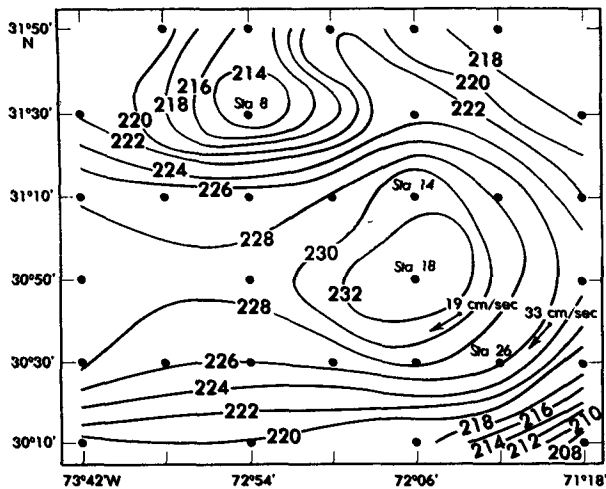


FIG. 1. Dynamic height anomaly (dyn cm) of the sea surface relative to 1800 db (dots represent CTD station locations).

Water samples were collected periodically to check CTD conductivity values. Final data processing included temperature and conductivity filtering to compensate for sensor mismatch and pressure sorting to 1 db intervals. A representative CTD profile plot is shown in Fig. 2.

3. Discussion

During the survey, shipboard data processing revealed a very peculiar CTD profile at Station 18 (Fig. 2). A layer of homogeneous water was observed between 690 and 840 m depth. An instrument malfunction was immediately suspected and it was not until the same feature had been detected in data from adjacent XBT profiles that the CTD profile

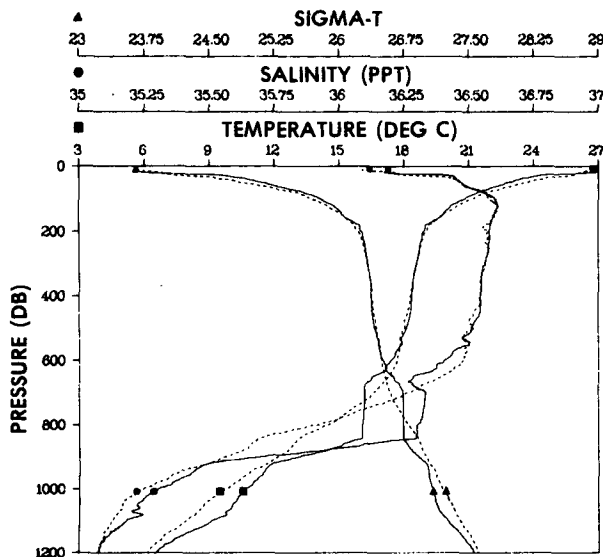


FIG. 2. CTD profiles at Stations 14 (dashed) and 18 (solid).

was accepted as valid. A second layer of reduced stability was seen at 1100 m. No other CTD profiles contained such a feature. An isothermal/isopycnal layer extending from 700 to 900 m depth was reported by Katz (1969) in the same area. He suggested that it may have been related to a front that was present at shallower depths.

The dynamic topography of the sea surface relative to 1800 db is shown in Fig. 1. Apparent is an anticyclonic eddy embedded in a larger anticyclonic feature. The eddy extends to a depth of ~1100 m. A small cyclonic eddy is evident near Station 8, but is not well resolved. There was evidence of a weak northeast-southwest thermal front near the surface similar to the one reported by Katz (1969) and Koshlyakov *et al.* (1979). Typical current speeds around the eddy implied by geostrophic calculations were 30 cm s<sup>-1</sup>, consistent with the current-meter data acquired in October near Station 26.

A north-south vertical section of  $\sigma_t$  is shown in Fig. 3.<sup>2</sup> The eddy is apparent below 300 m. The

<sup>2</sup>  $\sigma_t$  is used in this analysis rather than the more correct  $\sigma_\theta$ . For the depths involved, the difference is <0.02 units.

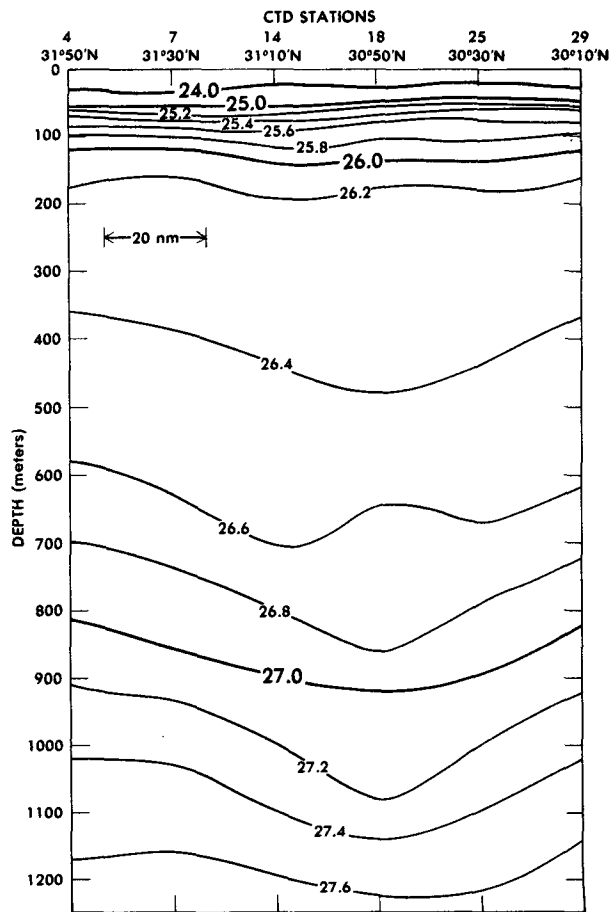


FIG. 3. North-south vertical section of  $\sigma_t$  along 30°50'N.

anomalous lens of homogeneous water was centered near Station 18 between the 26.6 and 26.8 isopycnals. The deeper layer of reduced stability occurred near  $\sigma_t = 27.1$ . Examination of CTD and XBT profiles near Station 18 revealed the horizontal extent of the lens to be  $\sim 40$  km east–west and less than 70 km north–south. XBT data indicated the presence of another deep isothermal layer on the western edge of the survey area.

XBT sections presented by Emery *et al.* (1980) show indications of weakly stratified and homogeneous lenses of water in the main thermocline. In the absence of salinity data it is not clear, however, what the density structures were in these cases. If it is assumed that the temperature profiles are representative of the density, as our observations suggest, the data of Emery *et al.* imply frequent occurrences of isopycnal lenses.

A temperature–salinity ( $T$ – $S$ ) diagram for the survey is presented in Fig. 4 (data are plotted at 10 m intervals). The significant anomalies associated with Station 18 are evident. The salinity maximum near 16°C, 36.3‰ occurred in the lens, which was neutrally stable. Excluding Station 18, salinity variability in the main thermocline was small for the survey. On the other hand, using data from a considerably larger area in which our survey was embedded, Ebbesmeyer and Taft (1979) found a relative maximum in the variability of salinity on  $\sigma_\theta$  surfaces in the interval 26.6–27.4. The  $T$ – $S$  anomalies of Station 18 in the isopycnal lens ( $\sigma_t \approx 26.75$ ) and at 1100 m ( $\sigma_t \approx 27.2$ ) fall in this interval, and are thus consistent with the overall variability of the region.

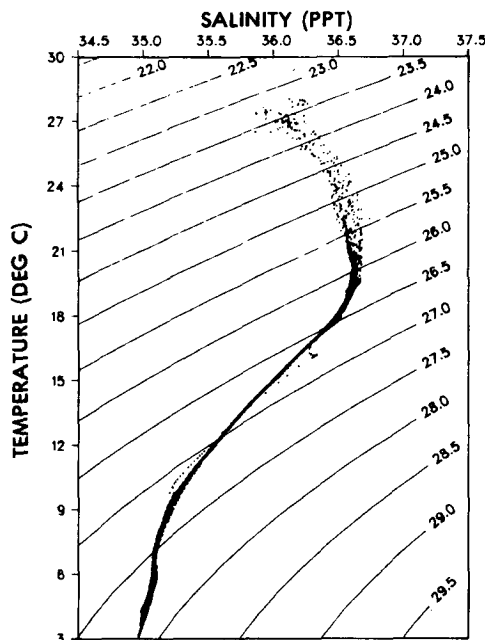


FIG. 4. Temperature–salinity diagram for survey. The anomalies near 16 and 10° are both due to Station 18.

The  $T$ – $S$  anomaly is indicative of intrusive, rather than linear mixing. There are no indications of an intrusive tongue, however; the peculiar profile was surrounded by “normal” profiles. It is possible that a thin tongue, such as that described by Gregg (1980), was missed by the coarse sampling pattern. Alternatively, the lens may have been trapped in the eddy at another location or time, perhaps by the pinching off of such a tongue. Indeed, the survey was conducted near the turning region of the westward Gulf Stream Return Flow (Reid, 1978; Ebbesmeyer and Taft, 1979) which transports warm, saline water of Mediterranean origin into the western Atlantic.

In a set of data similar to ours and from the same area, Koshlyakov *et al.* (1979) found an “interstitial intrusion” or lens of anomalous, nearly isopycnal water at a depth of  $\sim 200$  m. While this feature was shallower, warmer and more saline than the one we observed, its  $T$ – $S$  characteristics were quite similar and it was associated with an anticyclonic eddy and a surface front as well.

Closer examination of the vertical structure of the lens revealed weak, negative gradients in  $T$  and  $S$  with step structures from 5 to 15 m thick. These features were compensating since  $\sigma_t$  was constant in the lens. The details of the formation of the lens are not clear but some interesting points can be made. First, the remarkable vertical extent of water of virtually constant density suggests an ongoing or recent mixing process. Second, the salinity inversion at the top of the lens and the steppiness of  $T$ ,  $S$  within it suggest vigorous salt fingering in the main thermocline—a region already conducive to double-diffusive processes (Cooper and Stommel, 1968; Tait and Howe, 1968; Turner, 1973; Lambert and Sturges, 1977; Schmitt and Evans, 1978; Gregg and Sanford, 1980).

Isopycnal lenses of anomalous water may be far more common in the ocean than previously supposed (McDowell and Rossby, 1978), and may be quite significant in the mixing of water masses, vertically as well as laterally. When encountered during surveys of mesoscale features these lenses should be studied in such a way as to describe their time-evolution in three dimensions, on relatively small horizontal scales.

*Acknowledgments.* The authors thank Drs. J. P. Dugan, S. A. Piacsek and O. von Zweck for their helpful comments, Ms. D. Waters for drafting the figures, and Ms. D. Skipper for typing the manuscript.

#### REFERENCES

- Cooper, J. W., and H. Stommel, 1968: Regularly spaced steps in the main thermocline near Bermuda. *J. Geophys. Res.*, 73, 5849–5854.

- Ebbesmeyer, C. C., and Bruce A. Taft, 1979: Variability of potential energy, dynamic height and salinity in the main pycnocline of the western North Atlantic. *J. Phys. Oceanogr.*, **9**, 1073–1089.
- Emery, W. J., C. C. Ebbesmeyer and J. P. Dugan, 1980: The fraction of vertical isotherm deflections associated with eddies: An estimate from multiship XBT surveys. *J. Phys. Oceanogr.*, **10**, 885–899.
- Gregg, M. C., 1980: The three-dimensional mapping of a small thermohaline intrusion. *J. Phys. Oceanogr.*, **10**, 1468–1492.
- , and T. B. Sanford, 1980: Signatures of mixing from the Bermuda Slope, the Sargasso Sea and the Gulf Stream. *J. Phys. Oceanogr.*, **10**, 105–107.
- Katz, E. J., 1969: Further study of a front in the Sargasso Sea. *Tellus*, **21**, 259–269.
- Koshlyakov, M. N., Yu. D. Borisenko, A. L. Brekhovskikh, A. S. Vinogradov, V. N. Drozdov, K. V. Moroshkin, Yu. Kh. Pavel'son and D. G. Rzhaplinskiy, 1979: Synoptic oceanic fronts within the POLIMODE POLIGON (February–March, 1978). *Oceanological Researchers*, Vol. 31, POLIMODE Hydrophysical Expedition, U.S.S.R. Academy of Sciences, 42–55.
- Lambert, R. B., Jr., and W. Sturges, 1977: A thermohaline staircase and vertical mixing in the thermocline. *Deep-Sea Res.*, **24**, 211–222.
- McDowell, S. E., and H. T. Rossby, 1978: Mediterranean water: An intense mesoscale eddy off the Bahamas. *Science*, **202**, 1085–1087.
- Reid, J. L., 1978: On the middepth circulation and salinity field in the North Atlantic. *J. Geophys. Res.*, **83**, 5063–5067.
- Schmitt, R. W., and D. L. Evans, 1978: An estimate of vertical mixing due to salt fingers based on observations in the North Atlantic Central Water. *J. Geophys. Res.*, **83**, 2913–2919.
- Tait, R. I., and M. R. Howe, 1968: Some observations of thermohaline stratification in the deep ocean. *Deep-Sea Res.*, **15**, 275–280.
- Turner, J. S., 1973: *Buoyancy Effects in Fluids*. Cambridge University Press, 367 pp.

## A Note on Rotational and Divergent Eddy Fluxes

JOHN MARSHALL AND GLENN SHUTTS

*Atmospheric Physics Group, Imperial College of Science and Technology, London, England*

27 May 1981 and 9 September 1981

### ABSTRACT

If the deviation of mean flow from mean temperature contours is small, it is shown that a part of the eddy heat flux can be separated out which circulates around eddy potential energy contours, and has a component up/down the mean temperature gradient if there is flow advection of eddy potential energy into/out of the region. If the mean flow is strong, this rotational flux is large and results in regions of up- and downgradient flux. It is a prominent feature of maps of geostrophic eddy fluxes in the ocean and atmosphere.

### 1. Introduction

In baroclinically unstable flow, average eddy heat fluxes must have a net component down the mean gradient in order that mean available potential energy may be released. Similarly, quasi-geostrophic potential vorticity fluxes must have a net component down the mean potential vorticity gradient to offset dissipation of the eddy enstrophy (see Holland and Rhines, 1980; Rhines and Holland, 1979; Rhines, 1979). However, locally this association between mean gradient and eddy flux is not so strong (in regions where mean flow is large), because the sense of the eddy fluxes reflects not only the generation of eddies but also their decay downstream. Eddy fluxes in the atmosphere (Lau, 1978; Lau and Wallace, 1979, hereafter LW) and ocean (Holland and Rhines, 1980, hereafter HR) often have large rotational parts with both up- and downgradient components. Here it is shown that it is a rotational part of the eddy heat flux, circulating

around eddy potential energy contours, that represents the spatial growth and decay of eddies, and balances the mean flow advection of eddy potential energy.

### 2. Up- and downgradient eddy fluxes

The steady-state eddy potential energy equation (see HR) relates the flux of heat across the mean temperature gradient  $\overline{v'T'} \cdot \nabla \bar{T}$ , to the rate of conversion of eddy potential energy to eddy kinetic energy  $\overline{w'T'} \partial \bar{T} / \partial z$ , and the advection of eddy potential energy by the flow  $\overline{v \cdot \nabla T'^2/2}$ . It can be written, neglecting sources and sinks of heat and the advection of eddy potential energy by the eddy velocity,

$$\overline{v \cdot \nabla} \frac{\overline{T'^2}}{2} + \overline{v'T'} \cdot \nabla \bar{T} + \overline{w'T'} \frac{\partial \bar{T}}{\partial z} = 0, \quad (1)$$

where  $v$  is the horizontal velocity,  $w$  the vertical velocity and  $T$  is the temperature (taken proportional to the density). The overbar represents a time-average long compared to an eddy life time, and prime the deviation from the average.

In baroclinically unstable regions, loss of eddy